# We are IntechOpen,
## the world's leading publisher of Open Access books
## Built by scientists, for scientists

**6,900**
Open access books available

**185,000**
International authors and editors

**200M**
Downloads

**154**
Countries delivered to

Our authors are among the

**TOP 1%**
most cited scientists

**12.2%**
Contributors from top 500 universities

CLARIVATE ANALYTICS
**BOOK CITATION INDEX**
INDEXED

**WEB OF SCIENCE**™

Selection of our books indexed in the Book Citation Index
in Web of Science™ Core Collection (BKCI)

## Interested in publishing with us?
## Contact book.department@intechopen.com

# Plasma Switching by Laser Ablation

Ryosuke Hasegawa, Kazunori Fukaya and Akiyoshi Matsuzaki[1]
*Mie University*
*Japan*

## 1. Introduction

Plasma offers great potential for materials science [Lieberman & Lichtenberg, 2005]. Many interesting materials have been synthesized through plasma such as chemical vapour deposition (CVD). Besides, plasma etching is also known as one of the significant techniques utilizing plasma. In general, plasma is generated by direct electrical discharges of gases. On the other hand, we recently found a new method to form *pulse* plasma in an electric field *lower* than that necessary for the plasma formation by the direct discharges [Nakano et al., 2010; Tanaka et al, 2003a, 2003b, 2004]; the laser ablation of metals switches plasma formation and extinction alternately. We call this phenomenon PLASLA (plasma switching by laser ablation) and the plasma formed by this method PLASLA (plasma switched by laser ablation). The facts that PLASLA is the pulse plasma completely synchronized with laser ablation and can be formed in a lower electric field suggest PLASLA as a promising metal-catalysis reaction for materials science. For instance, the former fact suggests that we will be able to set the most suitable conditions for materials synthesis by appropriately integrating the ablation laser and the laser for the photochemical reactions and controlling their timing. As for the latter fact, the lower discharge potential of PLASLA can exclude the discharge of impurity gases. Furthermore, our previous experiments indicate that the products of the PLASLA reactions are different in the presence and absence of a magnetic field [Nakano et al., 2010]. In the present manuscript, as well as the overview of our previous study on PLASLA, we discuss PLASLA, focusing on its spatial discharge patterns and temporal waves. These ordered structures are of great interest, since plasma is a nonlinear process.

## 2. Generation and properties of PLASLA

Since the details of the systems and procedures of PLASLA experiments are described in the previous papers [Nakano et al., 2010; Tanaka et al, 2003a, 2003b, 2004], here we describe how to generate PLASLA with its main properties.

### 2.1 Generation of PLASLA

As schematically shown in Fig. 1(a), in a reaction chamber filled with $CF_4$ at a pressure of 0.2 Torr, with the laser ablation of Cu by the irradiation of a spinning Cu target with the fundamental beam of a $Nd^{3+}$:YAG laser (1.064 μm in wavelength, 45 mJ/pulse in power, 10

---

[1] Corresponding Author

Hz in repetition rate), after increasing a direct-current electric field applied between the parallel Cu plates of electrodes, stable PLASLA is formed at an electric field of 400 V, which is inadequate to form DC-plasma (direct current plasma), which is formed by the direct discharge at a potential of 500 V without laser ablation. The oscilloscope trace of PLASLA luminescence signal in Fig. 1(b) indicates that plasma is formed by the first laser ablation, quenched by the next ablation, formed again by the third ablation, quenched again by the fourth ablation, and so on, indicating that the PLASLA formation and quenching completely synchronize with laser ablation.
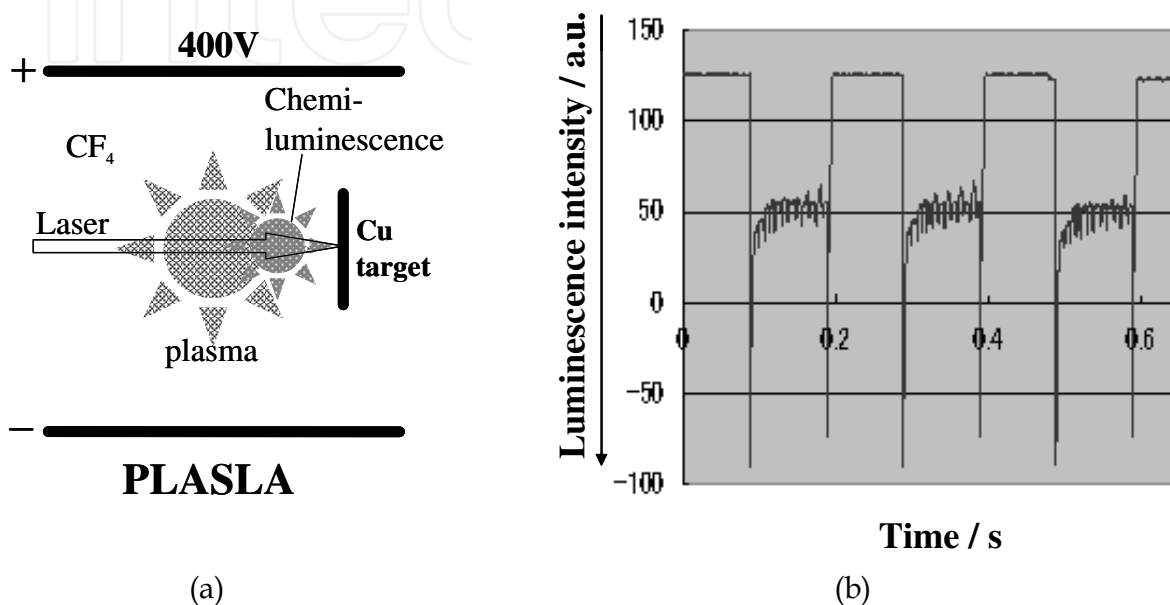


(a)                                                                                          (b)

Fig. 1. (a) The schematic illustration of the PLASLA experimental system. (b) The oscilloscope trace of PLASLA luminescence signal.

## 2.2 Properties of PLASLA

In PLASLA, the plasma can be obtained under milder conditions, since the laser ablation of metals induces the plasma in an electric field lower than that for the direct discharge in DC-plasma, suggesting the availability of the new products different from the ones of the DC-plasma. This also makes us possible to avoid the discharge of impurity gases with their low ionization potentials. For instance, in case that a minor constituent $N_2$ gas as the impurity discharges instead of the main constituent $CF_4$ gas in DC-plasma, it can be avoided in PLASLA, in which a $CF_4$ gas discharges as a predominant process in the same experimental system [Nakano et al., 2010]. Since the PLASLA plasma is the pulse completely synchronizing with laser ablation, the collaboration between the ablation laser and the laser for photochemical reactions will offer great potential for new materials syntheses.

The products of PLASLA in the gaseous Cu-$CF_4$ system are found to be polymeric carbon materials by time–resolved luminescence spectroscopy [Tanaka et al., 2003a, 2003b, 2004] and TOF (time-of-flight) mass spectrometry [Takenaka et al. unpublished data, Nakano et al., 2010]. Since various polymeric carbon materials have been extensively used for manufactures, PLASLA will be very promising in industry, as well as materials science.

PLASLA has been confirmed to form in a $CF_4$ gas through the laser ablation of various metals, i.e., Cu, Al, Ag, Zn, Co, Ni, Ti, Mo, and W [Nakano et al., 2010]. In view of the electronic configurations, these metals can be classified into three groups: Al, Cu, Ag, and Zn in Group-1, Co and Ni in Group-2, and Ti, Mo, and W in Group-3. The configurations in Group-1 are $s^2p^1$ in Al, $d^{10}s^1$ in Cu, $d^{10}s^2$ in Zn, and $d^{10}s^1$ in Ag, and have the closed highest inner sub-shells. The configurations in Group-2 are $d^7s^2$ in Co and $d^8s^2$ in Ni, and have the greater-than-half-filled highest inner sub-shells. The configurations in Group-3 are $d^2s^2$ in Ti, $d^5s^1$ in Mo, and $d^4s^2$ in W, and have the less-than-or-equal-to-half-filled highest inner sub-shells. On the other hand, we have experimentally found that PLASLA is most stable in Group-1, middle in Group-2, and least in Group-3 [Nakano et al., 2010], suggesting that neutral chemical reactions compete with the PLASLA plasma reactions in Groups-2 and 3 metals, since they have open highest inner sub-shells. For instance, we have confirmed that the PLASLA formation rate is fastest in Group-1, middle in Group-2, and slowest in Group-3; that the PLASLA extinction time is longest in Group-1, middle in Group-2, and shortest in Group-3.

We have found the various interesting facts on the interaction of PLASLA with a magnetic field [Nakano et al., 2010]. The magnetic field effects on PLASLA are due to the magneto-hydro-dynamics (MHD) processes and the magnetic effect on the chemical reactions. The main MHD processes in PLASLA are the $\mathbf{E}$x$\mathbf{B}$ drift and the cyclotron circulation of ions and electrons. These processes increase the PLASLA potential, at which PLASLA is formed, and the activation energy of PLASLA plasma reactions, since they interrupt the movements of ions and electrons for the plasma chemical processes. As a magnetic field increases the PLASLA potential, the shape of PLASLA pulse varies considerably. By the analysis of the magnetic field effect on the activation energy of PLASLA, it is found that a magnetic field increases the activation energy of the charge-transfer processes and decreases that of the ionic chemical reactions accompanying chemical-bond cleavages. The TOF-mass spectrometry shows that the PLASLA product materials formed in a magnetic field are different from those of zero-field PLASLA. That is, for PLASLA in a magnetic field, the detected carbon clusters are rather small in size and are free from impurities such as metals and fluorine.

Thus, in view of materials science, PLASLA is a promising metal-catalysis reaction.

## 3. PLASLA discharge pattern

In this section, we study the mechanism of PLASLA by quantitative analysis of PLASLA discharge patterns with various metal targets.

### 3.1 Discharge pattern imaging

The upper panel in Fig. 2 shows the present imaging system. The lower panel in this figure shows the typical images of DC-plasma, laser ablation (CuF chemiluminescent reaction), PLASLA with a Cu target. In DC-plasma, bright plasma sheaths are formed around the electrodes. In the laser-ablation image, the bright sphere of CuF chemiluminescence is observed near the Cu target. In PLASLA, the bright plasma sheaths around the electrodes and the bright sphere of CuF chemiluminescence near the Cu target are observed.

**Imaging system**

**Laser**

**Focus lens**  **Electrodes**  **Spinning metal target**

**Observed images with a Cu target**

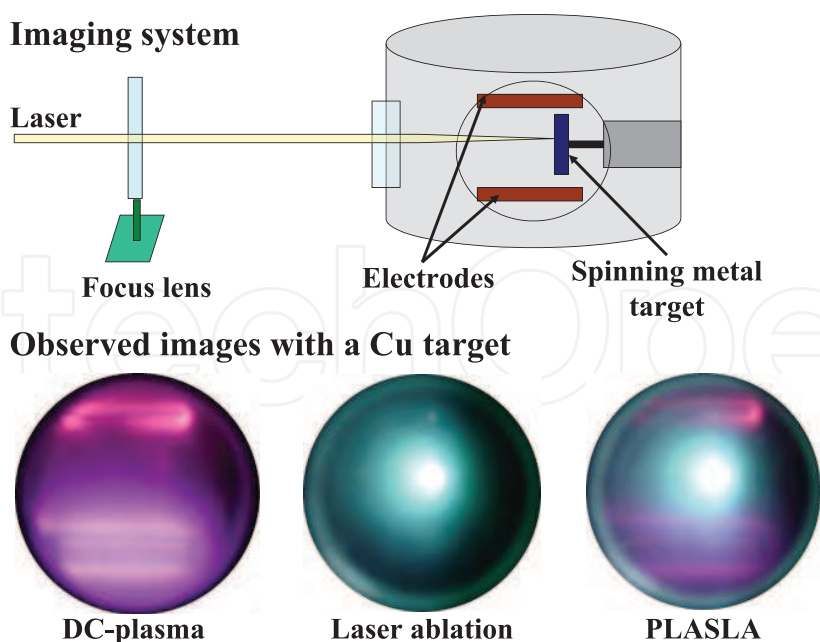DC-plasma      Laser ablation      PLASLA

Fig. 2. Upper panel shows the imaging system. Lower panel shows the observed images of DC-plasma, laser ablation (CuF chemiluminescent reaction), and PLASLA.

### 3.1.1 PLASLA discharge patterns with various metals

Figure 3 shows the PLASLA discharge patterns with various target metals. PLASLA can be formed with all these metals. The deformation of the sheaths is evident in the discharge patterns of the Ti, W, and Mo targets. These target metals have been classified into Group-3, having electronic configurations of $d^n s^2$ ($n \leq 5$), where the electronic configurations are $d^{10}s^1$ ($d^{10}s^2$ for Zn) in Group-1 metals and $d^n s^2$ ($n>5$) in Group-2 metals. Such deformation cannot be observed in other metals. We suppose that the deformation is closely related to the fact that PLASLA is rather unstable with Group-3 metals. As a mechanism for the unstable PLASLA with Group-3 metals, the competition of plasma ionic chemical processes with neutral radical chemical processes is suggested from the electronic configurations [Nakano et al., 2010]. Furthermore, the figure indicates that the PLASLA potentials are rather low, middle, high in Group-1 metals (Ag, Al, Zn, Cu), Group-2 metals (Co, Ni), and Group-3 metals (Ti, W, Mo), respectively. The same mechanism as that for the PLASLA stability has been proposed for the fact [Nakano et al., 2010].

Figure 4 shows the distributions of PLASLA luminescence intensity near electrodes for Cu and Ti targets. As shown in Fig. 4(a), Regions 1-4 are set on the PLASLA discharge image. After the colour of the images is converted to grey-scale ones, the luminescence intensity is expressed in terms of a lightness scale from 1 to 25, as shown in Fig. 5. Thus, the PLASLA luminescence intensities in Regions 1-4 outside and inside the reaction site near electrodes are shown in Figs. 4(b) and (c) for Cu and Ti targets, respectively. While the distributions in Regions 1-4 are very similar between Cu-PLASLA and Ti-PLASLA inside the reaction sites near the anodes, they are evidently different outside the reaction site. In Cu-PLASLA, the distributions are rather flat over Regions 1-4 outside the reaction site, while the luminescence intensity is low in Regions 1 and 2 and steeply increases from Region 3 to Region 4 outside the reaction site in Ti-PLASLA. These results are evident from the images
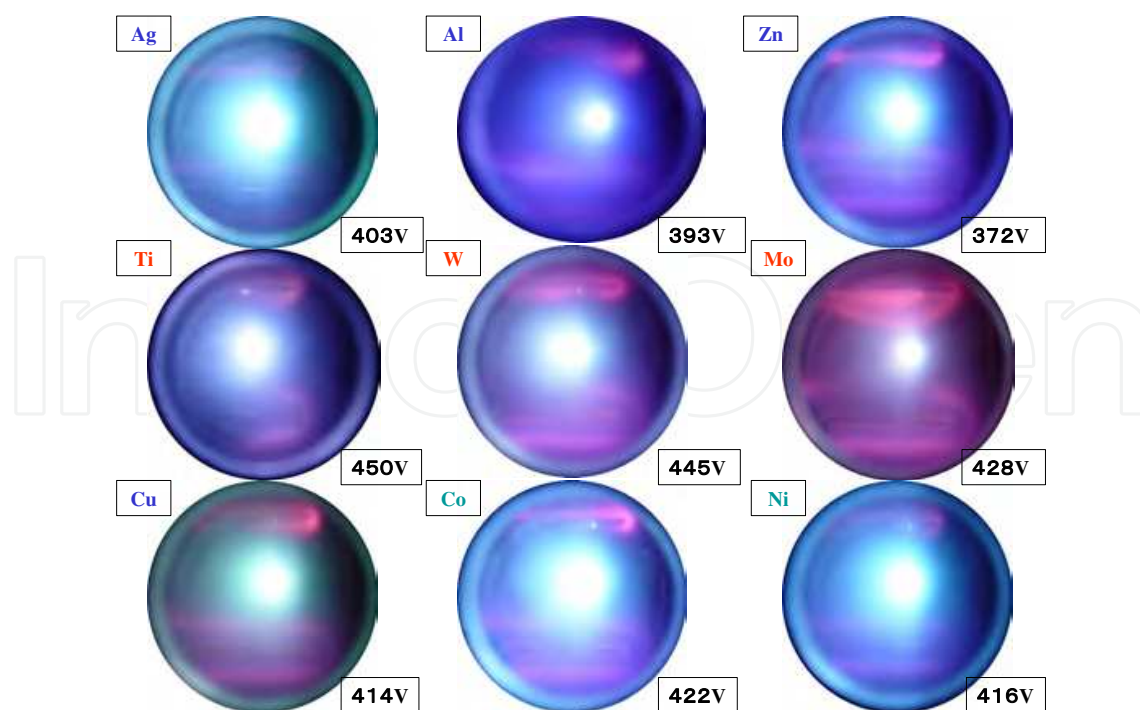
Fig. 3. PLASLA discharge patterns with various target metals. Metals and PLASLA potentials are indicated on the upper-left sides and lower-right sides of discharge images, respectively. The colours indicating metals are classifying them into groups: Group-1 is in blue, Group-2 in green, Group-3 in red.

of Cu-PLASLA and Ti-PLASLA discharge patterns in Fig. 3. This figure indicates that the stable sheaths are formed around electrodes in Cu-PLASLA, while the sheaths around the electrodes are completely quenched in Regions 1 and 2 in Ti-PLASLA. Furthermore, the sheaths peel off the electrodes in Ti-PLASLA. These facts indicate that there is a diference in the chemical processes between Cu-PLASLA and Ti-PLASLA, suggesting the additional chemical processes in Ti-PLASLA. We suppose that this additional chemical processes are the neutral radical reactions competing with the plasma ionic reactions.

The discharge image of Cu-PLASLA in Fig. 3 and its luminescence intensity distribution in Fig. 4(b) indicate that the stable, undeformed sheaths are formed arounds the anode and the cathode in Cu-PLASLA, yet the plasma luminescence disappears only in Regions 1-3 on the reaction site of the anode, suggesting that significant chemical processes occur in this area. The similar quenching of the plasma luminescence in Regions 1-3 on the reaction site of the anode is observed in the discharge patterns of Al-, Co-, Ni-PLASLA, as shown in Fig. 3.

### 3.1.2 PLASLA discharge patterns between Cu electrodes

In this section, we discuss the Cu-PLASLA discharge pattern between the electrodes. For the analysis, the 25 x 4 grid was set on the discharge pattern images, as shown in Fig. 5. Then the images were transformed from colour to grey-scale ones. Then, the lightness of the areas in the grid on the grey-scale images was transferred to the 1-25 quantities with use of the scale, as shown in Fig. 5. Four columns of the grid are named Regions 1-4, as shown in this figure.
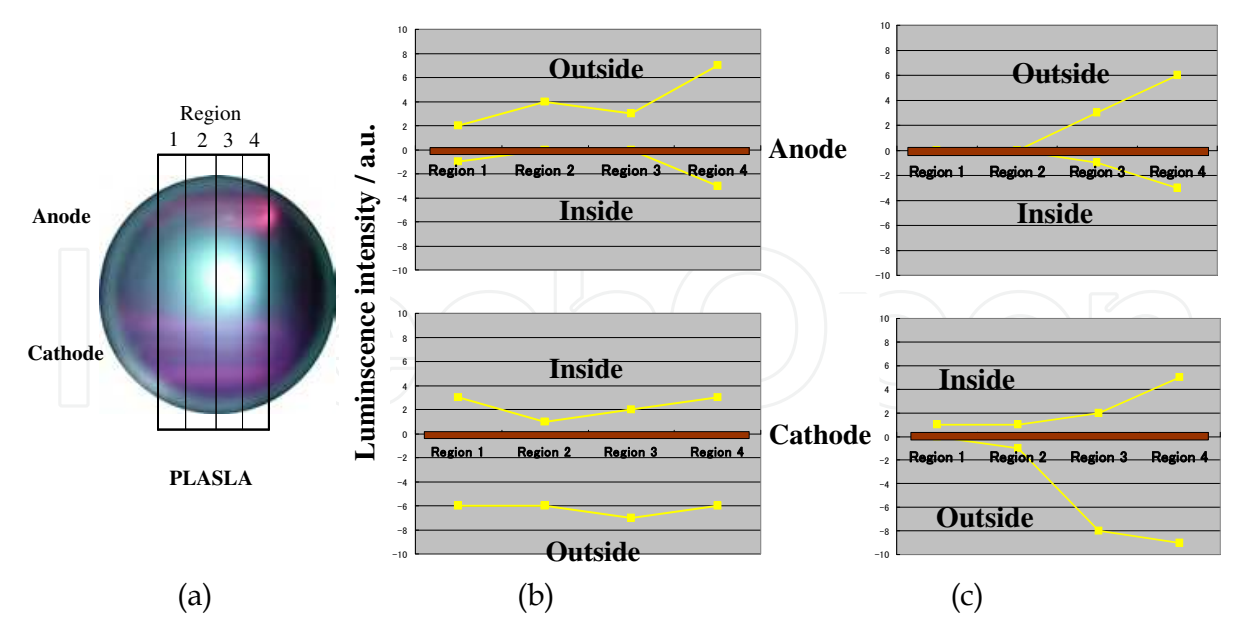
Fig. 4. Luminescence intensity distributions near electrodes in Regions 1-4, evaluated from PLASLA discharge patterns. (a) Regions 1-4. (b) Cu target. (c) Ti target.

The results of the analysis are shown in Fig. 6. In this figure, the luminescence intensity is plotted as a function of distance from the cathode in Regions 1-4 for DC-plasma, Laser ablation (CuF-chemiluminescent reaction), and PLASLA images. In the abscissa, the positions of the cathode and the anode are at 0 and 3.5 cm, respectively. In DC-plasma, the figure indicates that the sheath around the cathode is very stable and the luminescence intensity constantly decreases from the cathode to the anode. As for the resemblance among the curves in Regions 1-4, they are completely same in the area from the cathode to the anode, while there are clear differences only near the anode, indicating the differences in the sheaths on the anode. The fact that the sheaths around the anode greatly vary in Regions 1-4 is probably due to the difference in the stability in the spatial distribution of ions and electrons.
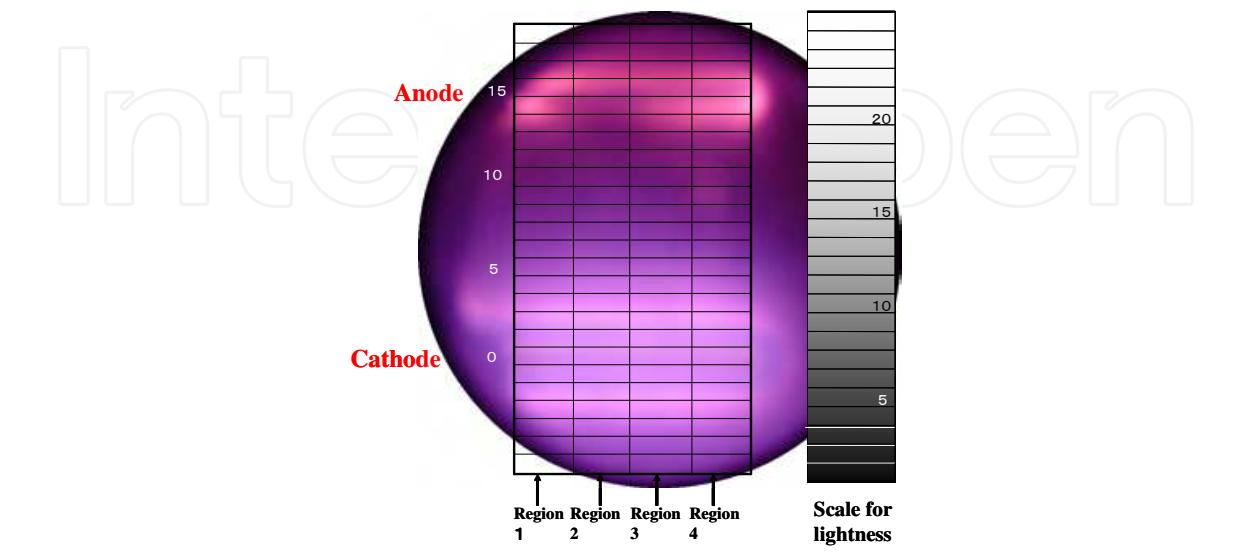


Fig. 5. Grid on the discharge pattern with the lightness scale for the analyses in Fig. 6.
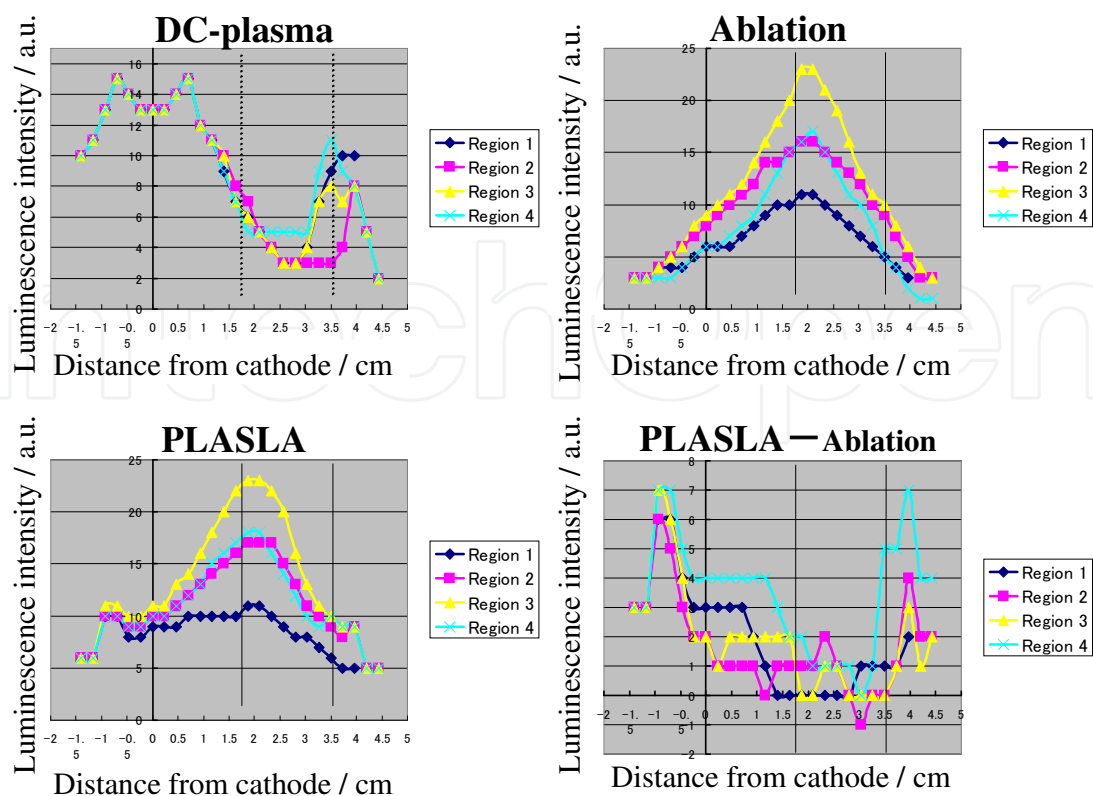
Fig. 6. Luminescence intensities between electrodes in DC-plasma, Ablation (CuF chemi-luminescence), PLASLA, and the difference in the luminescence intensity between the PLASLA and laser-ablation patterns.

In Ablation (laser ablation), the image is essentially spherical, but it is evidently extended in the flight direction of laser-ablated Cu atoms. Since the image of PLASLA includes the laser-ablation luminescence as well as the plasma luminescence of PLASLA, the latter image is extracted by subtracting the former image from the PLASLA image, as shown in the right-bottom panel of the figure. As compared with the image of DC-plasma, the luminescence intensity between the electrodes is largely reduced in this subtraction image, i.e., the plasma luminescence image of PLASLA, suggesting the more enhanced chemical reactions. The quenching is greatest and spatially widest in Regions 2, 3 and 1. The quenching in Region 4 is rather small in the inside site on the cathode and is rather large in the inside region on the anode. Furthermore, while the sheath completely surrounds the anode in DC-plasma, it is quenched in the inside site on the anode in the plasma luminescence image of PLASLA, indicating the additional chemical reactions in PLASLA. Thus the present image analysis has found that the plasma reaction occurs with laser-ablated metal atoms widely between the cathode and the anode in Regions 2, 3, and 1. The study on the product materials deposited on the electrodes will help us for the further discussion.

## 4. Product materials attached to the electrodes

Product materials deposited on the electrodes were stored in four bottles as samples by separately collecting the materials from the both sides of the cathode and the anode after careful observation of their colours one by one in each PLASLA experiment. The results are shown in Table 1 and in Fig. 7.

| Metals | Anode/ inside | Anode/ outside | Cathode/ inside | Cathode/ outside |
|--------|---------------|----------------|-----------------|------------------|
| **Ag** | B, 4 | B, 1 | None | None |
| **Al** | B, 4 | B, 2 | B, 4 | None |
| **Zn** | 1 | None | B, 1 | None |
| **Ti** | B, W, 2 | W, 4 | None | None |
| **W** | B, 2 | None | None | None |
| **Mo** | B, 2 | None | None | None |
| **Cu** | B, 4 | B, 4 | B, 1 | None |
| **Co** | B, 3 | W, 4 | B, 1 | None |
| **Ni** | B, 3 | B, 2 | B, 2 | None |

Table 1. The product materials attached to the electrodes for various metal targets. B and W indicate the black and white coloured materials, respectively. Numbers 1-4 and "none" indicate the amounts of product materials: 1 (a little) to 4 (very much) and "none" is 0.
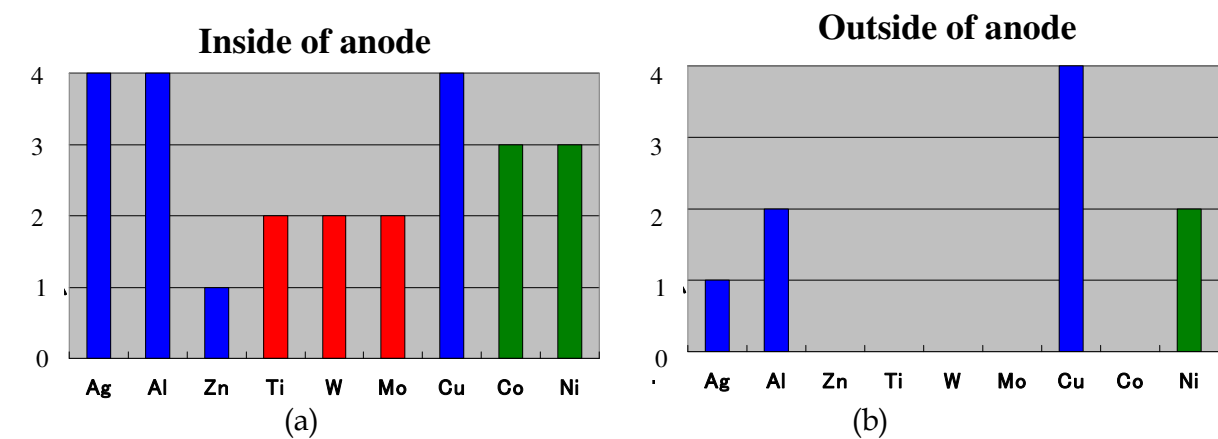


Fig. 7. The yields of carbon-like (black-coloured) product materials attached to the anode for various metal targets. In the ordinates, scales indicate the amounts of the product materials: 0 (none) to 4 (very much).

The results in Table 1 indicate that the yields of materials are evidently greater in the anode than in the cathode. Furthermore they are evidently greater in the reaction side of the both electrodes, i.e., between electrodes, than in another side. The main products on the electrodes are carbon-like (black-coloured) materials. Yet, besides the materials, white-coloured materials are yielded on the both sides of the anode in the Ti target and on the non-reaction side of the anode in the Co target. The white-coloured materials are yielded more in the non-reaction side of the anode than in its reaction side, while the black-coloured materials are more yielded in the reaction side of it. Figure 7, which shows the yields of carbon-like (black-coloured) product materials deposited on the anode for various metal targets, indicates that the carbon-like materials are yielded most in the targets of Group-1 metals, middle in the targets of Group-2 metals, and least in the targets of Group-3 metals. As described in the previous papers [Nakano et al., 2010], PLASLA is most stable in the target of Group-1 metals, middle in the targets of Group-2 metals, and least in the targets of Group-3 metals. This fact is due to the electronic configurations of the target metals [Nakano et al., 2010], which suggest that neutral chemical processes compete with the plasma

reactions of PLASLA in the targets of Groups-2 and 3 metals. Hence the white-coloured product materials on the anode with the Ti and Co targets are suggested to be the products of the neutral chemical reactions [Nakano et al, 2010]. This agrees with the fact that the white-coloured materials are more yielded on the non-reaction side of the anode in the Ti and Co targets, where the plasma reaction of PLASLA is inactive.

The PLASLA products materials will be discussed more in detail with the results of the TOF mass spectrometry and Time-resolved luminescence spectroscopy measurements [Takenaka et al., unpublished data].

## 5. Transient signal analysis of PLASLA formation and extinction

As shown in Fig. 1(b), the PLASLA luminescence is pulse, synchronized with laser ablation. The shape of the PLASLA luminescence pulse is studied. As shown in Fig. 8, the pulse shape in the PLASLA formation is found to be classified into two types: Type-A in Fig. 8(a) and Type-BC in Fig. 8(b). In Type-A, the PLASLA ignition pulse simply decays to the constant stable luminescence, while the overshoot labelled by B and C in Fig. 8(b) is found in Type-BC. Furthermore, it is found that Type-A is observed in PLASLA with Group-1 metal targets and Type-BC is done in PLASLA with Groups-2 and 3 metal targets. However, it should be noted that Type-A was once observed in PLASLA with the Ti target, while Type-BC is usual with the target. This fact suggests that the both types are due to the common mechanism and only depend on a parameter

Thus, as shown in Fig. 9, we made the simulation study for the time features of the PLASLA ignition by using a simple model, which is the combination of the signals of the ablation luminescence and the plasma luminescence as a function of delay of the latter signal from the former signal. The results indicate that their overall signal varies from Type-A to Type-BC with the delay between these signals. Hence it is found that the plasma luminescence signal appears rather immediately after the laser ablation for Group-1 metal target, while it is delayed rather more for Groups-2 and 3 metals target. That is, it takes more time for the plasma reaction in PLASLA with Groups-2 and 3 metals target. Thus it is found that PLASLA is formed more easily with Group-1 metal target than with Groups-2 and 3 metals target, as previously described [Nakano et al., 2010].
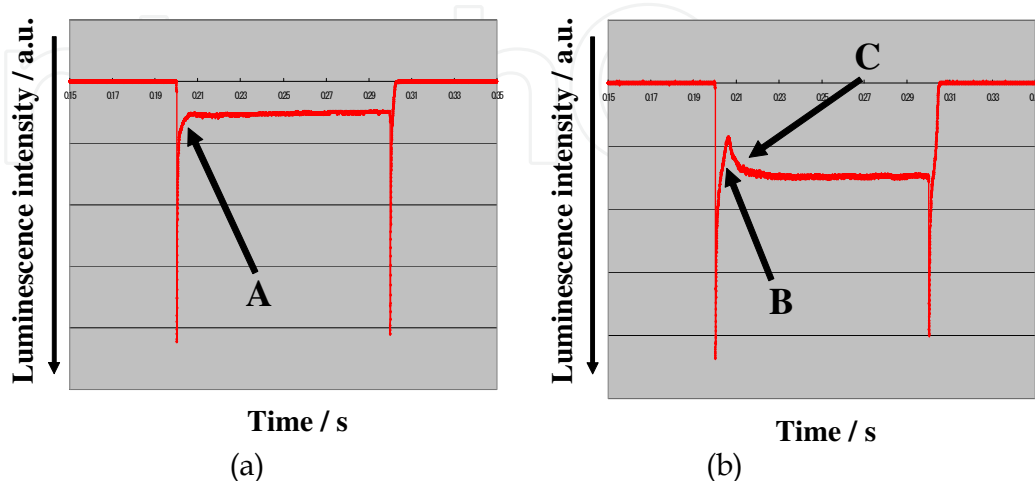


Fig. 8. The transient signals of PLASLA luminescence. (a) Type-A, (b) Type-BC, where targets: (a) Ag, (b) Ti.
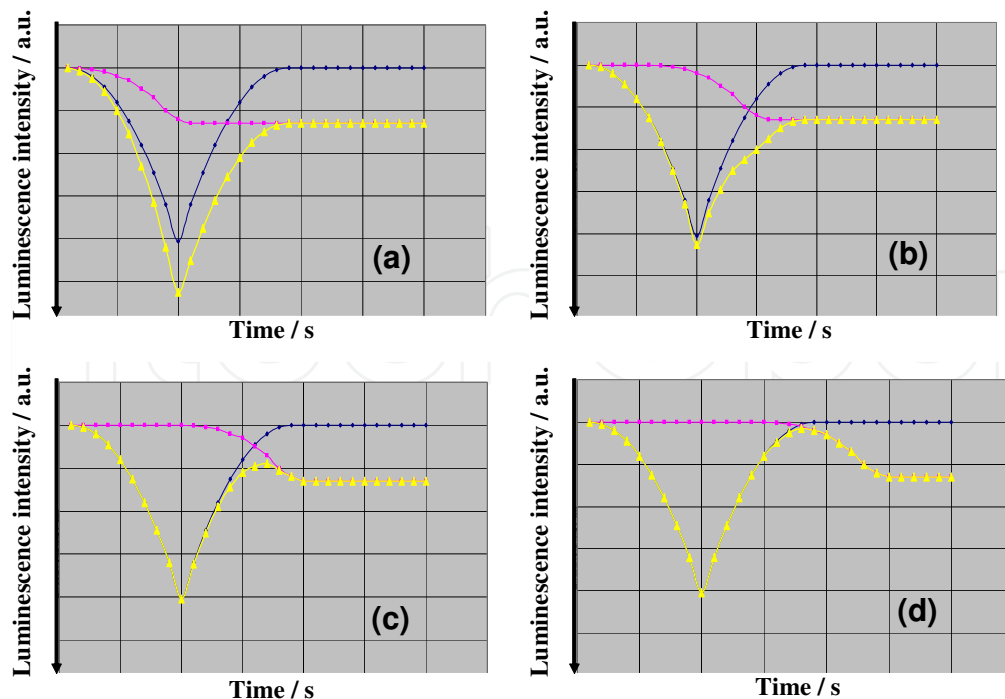
Fig. 9. The schematic illustration of the transient signals of PLASLA formation with ablation luminescence signals (blue), plasma luminescence signals (pink), and their overall signals (yellow) for various delays of the plasma signals, where the delay increases from (a) to (d).

As shown in Fig. 10(a), the decay rate of process C is found to correlate with the decay rate constant of process B for various target metals such as Al, Ni, Co, Ti, W, and Mo; the decay rate of process C exponentially increases with the decay rate constant process B. Hence it is evident that the Type-C process is the recovery process of the Type-B process. Furthermore, as described in the previous paper [Nakano et al, 2010], we have confirmed that the PLASLA formation rate in the Type-A process exponentially decreases with ionization potential of target metals and concluded that PLASLA starts from the sequent initial processes of $(M + e \rightarrow M^+ + e)$ and $(M^+ + CF_4 \rightarrow MF + CF_3^+)$, where M is the target metals.

On the other hand, the feature of the PLASLA pulse near the PLASLA extinction is shown in Fig. 10(b). The feature suggests that the PLASLA luminescence signal decays in the two steps probably with the sequence of two exponential decays. As described in the previous paper [Nakano et al, 2010], we also have confirmed that the PLASLA extinction time, which is defined as t in Fig. 10(b), increases with ionization potential of target metals and concluded that PLASLA is quenched through the process of $(M + CF_4^+ \rightarrow M^+ + CF_4)$, where M denotes the target metals. Thus the transient signal analysis of the PLASLA formation and extinction indicates that the features of the PLASLA pulse are due to the common mechanism for various target metals.

## 6. Chemical waves in PLASLA

Plasma is one of the ordered structures through the nonlinear processes. In fact, the spatial waves are observed in the PLASLA photo-images, as discussed in section 3. Besides these spatial waves, temporal waves will also be formed in PLASLA. In this section, we

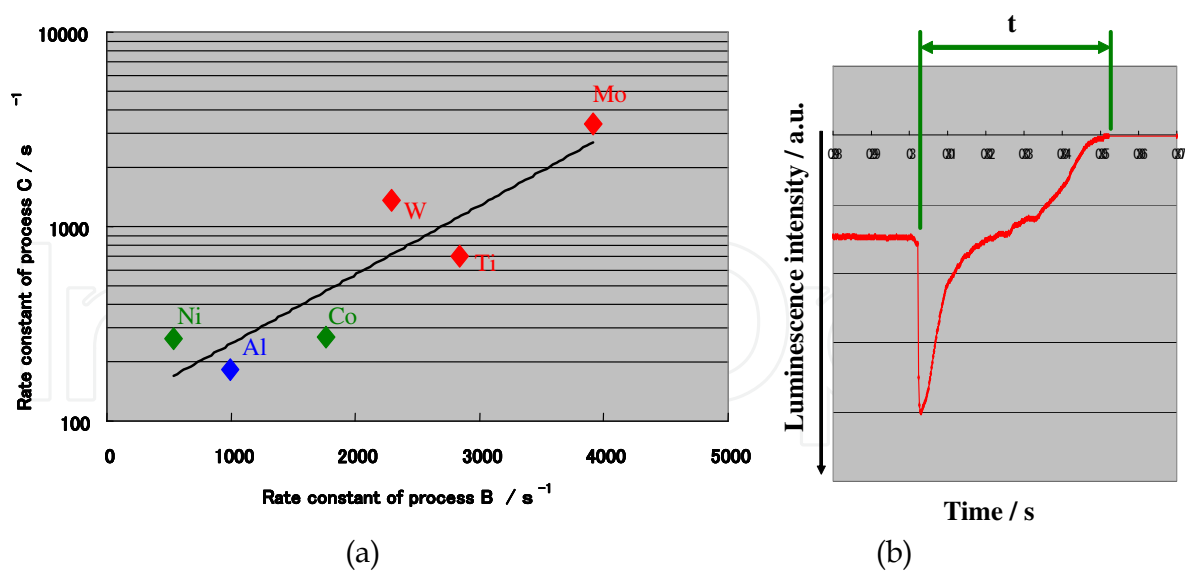(a)                                                    (b)

Fig. 10. (a) The plot of logarithmic rate constant of process C as a function of rate constant of process B in the Type-BC PLASLA formation. (b) Transient signal of PLASLA luminescence near the extinction, indicating the PLASLA extinction time t. (Target: Ni).

investigate the temporal waves in PLASLA for the gaseous Cu-CF$_4$ system by analysing the waves superimposed onto the pulsing time profile of PLASLA luminescence intensity.

## 6.1 Systematic waves in PLASLA

As shown in Fig. 1(b), the transient signal of PLASLA luminescence pulses. It is found that the systematic waves are superimposed onto the pulses, as shown in Fig. 11.
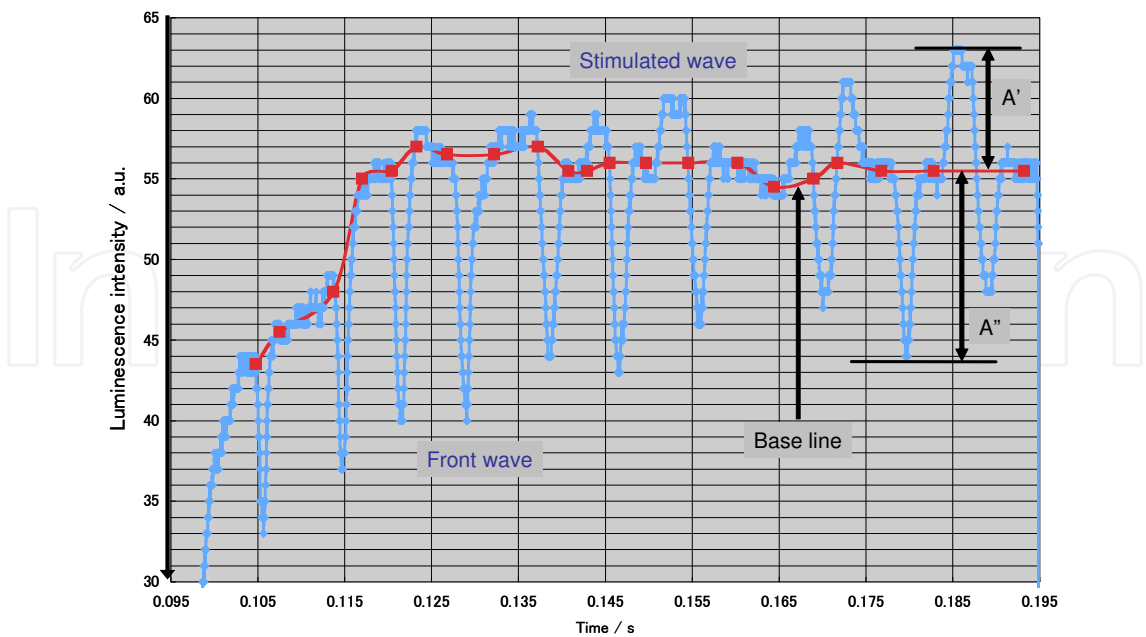


Fig. 11. Enlarged transient signal of PLASLA luminescence (Blue solid line) with the baseline (red solid line). A' and A" are the amplitudes of stimulated wave and front wave, respectively.

The figure indicates that the periodic front wave appears just after the laser ablation, increasing the luminescence intensity measured from the baseline. After that, the periodic stimulated wave appears, decreasing the luminescence intensity from the baseline in the front wave. In particular, its appearance is clear since 125 ms. The feature in Fig. 11 suggests that the laser ablation induces the front wave and then the front wave induces the stimulated wave to be a united wave. The baseline, which is indicated by a red line in this figure, largely varies before 125 ms and is constant after that.

In Fig. 12, the logarithmic amplitude of the front wave, which is defined by A″ in Fig. 11, is plotted as a function of time. The figure indicates that the amplitude of the front wave exponentially increases and then the decreases with time at rate constants of 23.2 and 10.1 s$^{-1}$, respectively, i.e., the growth rate of the front wave turns out to be twice faster than the decay rate. The turning-point region for the growth and decay of the front wave, which is shown by the green belt in Fig. 12, completely coincides with the region, where the baseline becomes constant.
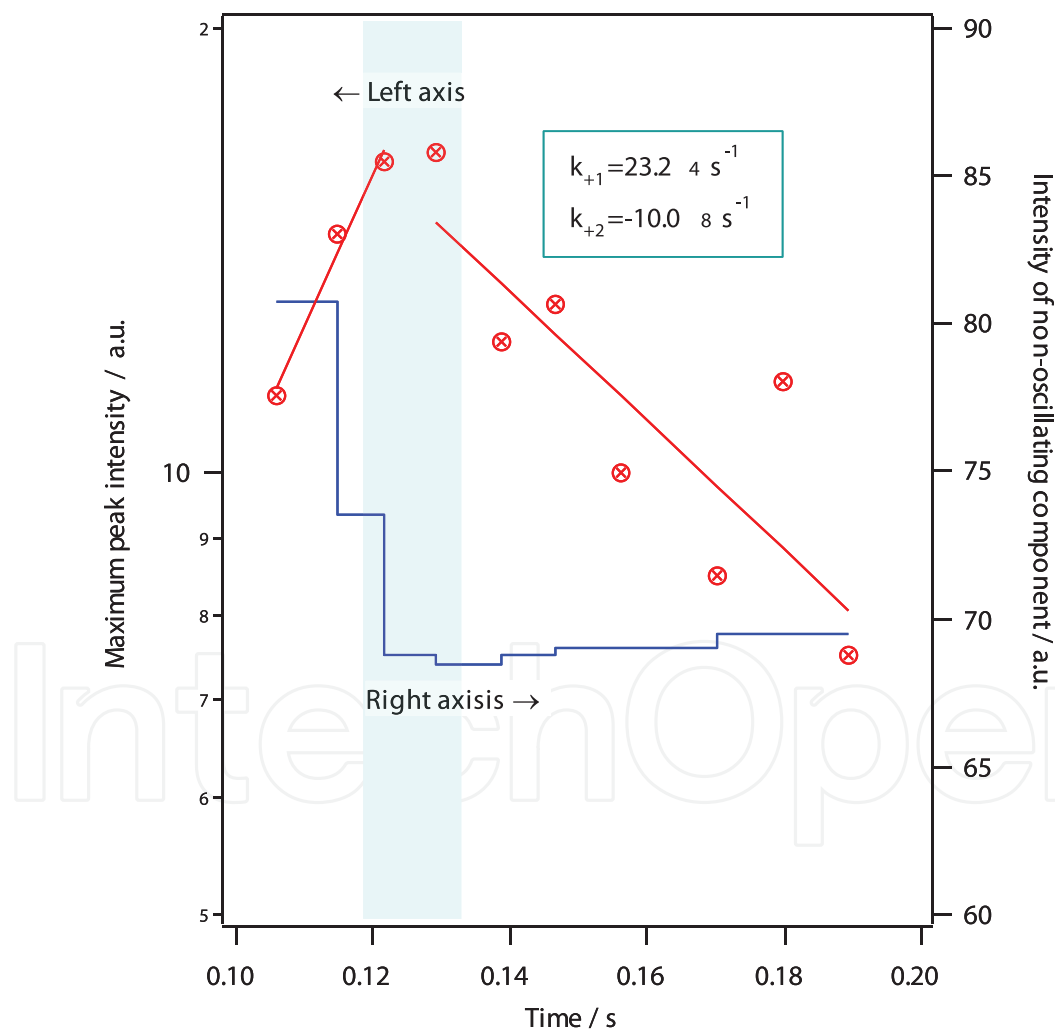


Fig. 12. Plot of the amplitude of the front wave, which is defined by A″ in Fig.11, as a function of time for the left ordinate. The blue solid line is the baseline, which is shown by a red line in Fig. 11, for the right ordinate. The green belt near 0.12-0.13 s indicates the turning point for the growth and decay of the front wave.

Figure 13 indicates the plot of the logarithmic amplitude of the stimulated wave, which is defined by A' in Fig. 11, as a function of time. The amplitude of the stimulated wave also exponentially increases with time. The growth rate constant of the stimulated wave turns out to be 34.9 s⁻¹, which is faster by 3.5 than the decay rate constant of the front wave. Hence it is found that the change in the system is rather rapid just after the laser ablation to form the front wave, which approaches to a steady oscillation rather slowly after that, inducing the stimulated wave, which grows rather faster to be combined to the united wave with the front wave. Thus, when the front wave and the stimulated wave converge on the united wave, the rates of the changes in their amplitudes are different, while they have essentially the common period.
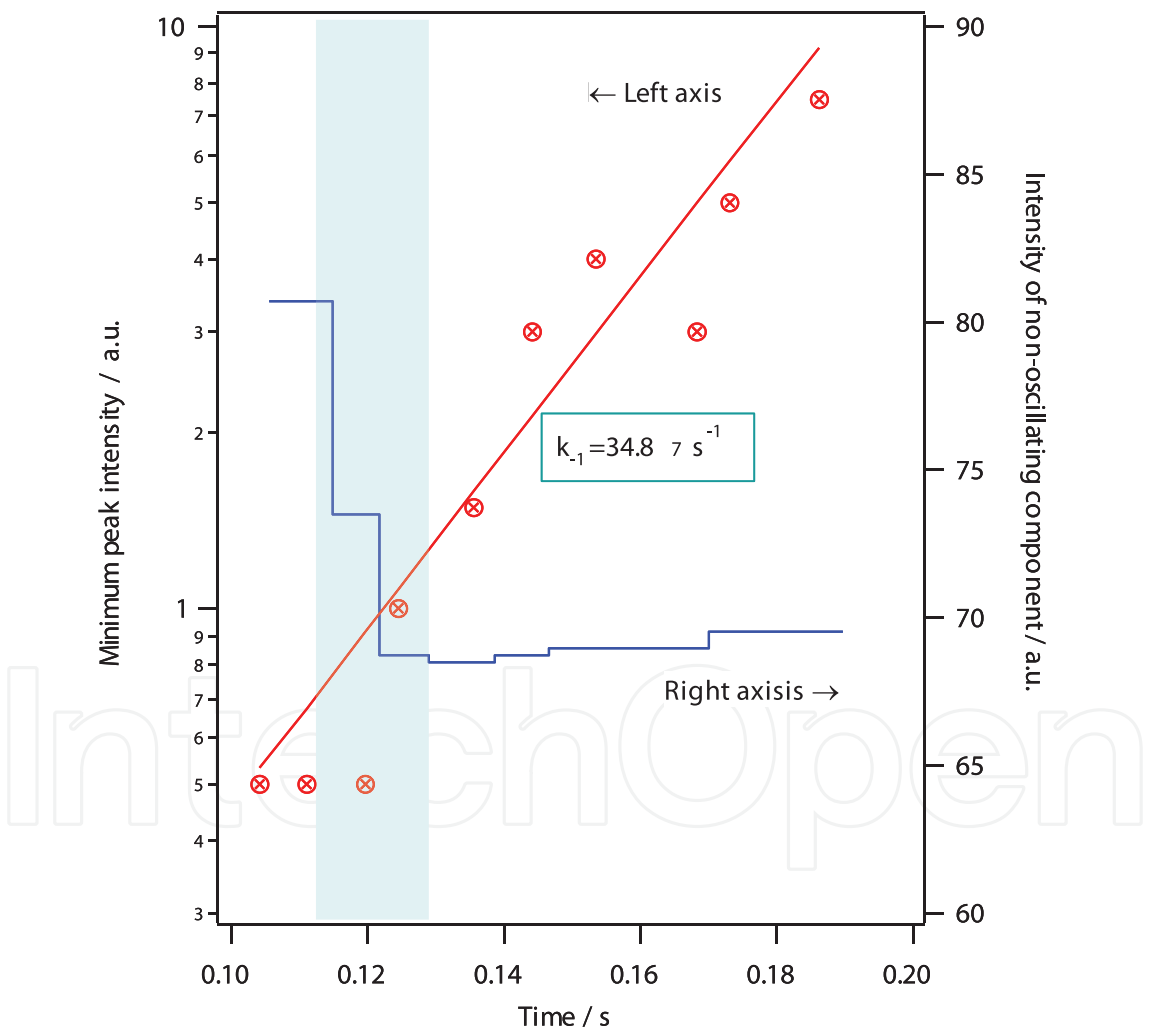


Fig. 13. Plot of the amplitude of the stimulated wave, which is defined by A' in Fig.11, as a function of time for the left ordinate. The blue solid line is the baseline, which is shown by a red line in Fig. 11, for the right ordinate. The green belt near 0.12 s indicates the turning point for the baseline to become constant.

In Fig. 14, the total intensity, which is defied as the sum of the amplitudes of the front and stimulated waves, is plotted as a function of time. The figure indicates that the intensity linearly increases with time, expressed in terms of (amplitude = 13.9 + 8.4t), where t is time in s of its unit. The feature of the total peak intensity as a function of time suggests that the front wave and the stimulated wave are united to be a single wave, amplitude of which slightly increases with time.
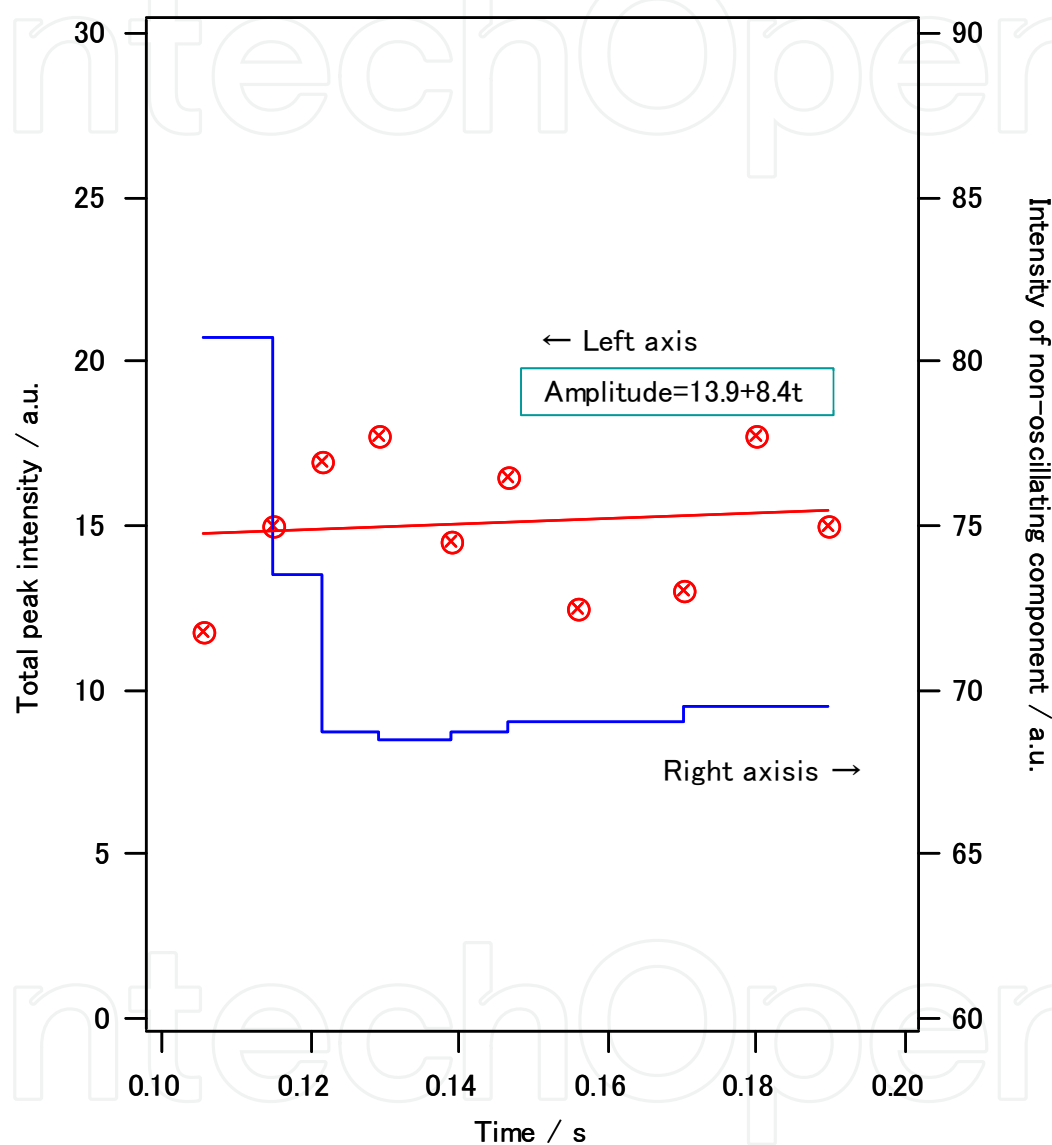


Fig. 14. Plot of the sum of the amplitudes of the front and stimulated waves, which are defined by A″ and A′ in Fig.11, as a function of time for the left ordinate. The blue solid line is the baseline, which is shown by a red line in Fig. 11, for the right ordinate.

The fact that the front and stimulated waves are united is evident also in Fig. 15; as the mid-point of the amplitudes of these waves converges to zero, the amplitudes of these waves become equal. The figure indicates that the front and stimulated waves appear alternatively. The periods of these waves fluctuate and the fluctuation is rather large in the stimulated wave.

This change in the PLASLA system is schematically illustrated in Fig. 16. At the initial point, the front wave is generated by laser ablation, grows after that, and is united with the stimulated wave to be transformed into a steady-state oscillation. Thus, by the study in this section, it is found that the waves generated in PLASLA have the systematic characteristics.
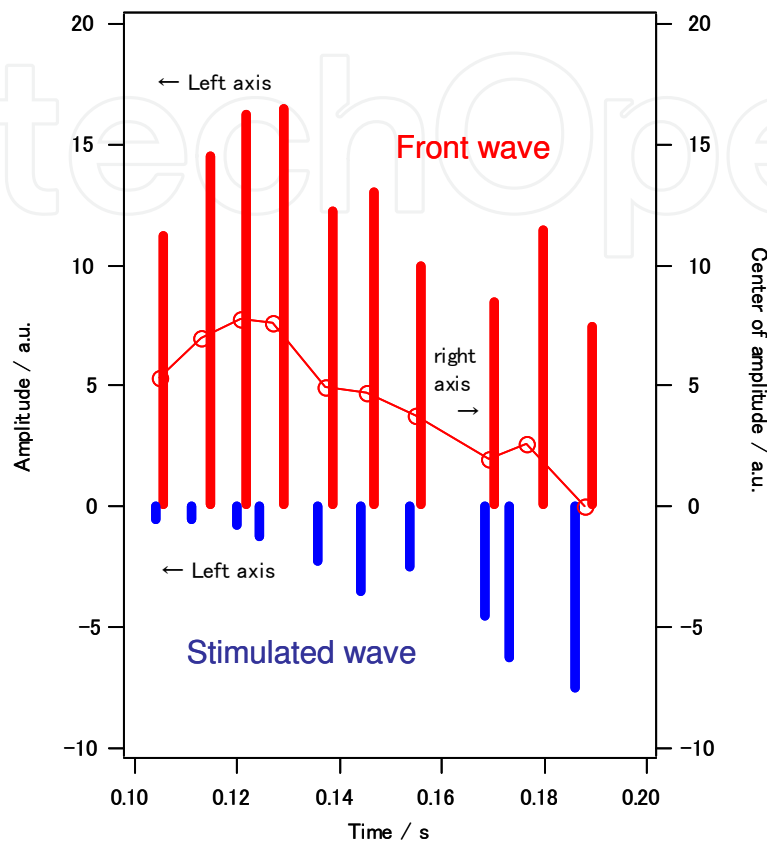


Fig. 15. Plot of the amplitudes of the front and stimulated waves, which are defined by A″ and A′ in Fig.11, as a function of time for the left ordinate. The red solid line is the mid-point of the sum of the amplitudes of the front and stimulated waves, plotted for the right ordinate.
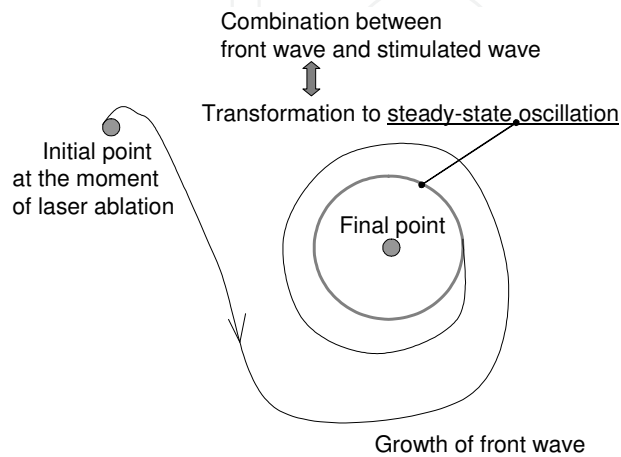


Fig. 16. Schematic illustration of the change in the PLASLA system, where, after the front wave generation by the laser ablation, the front wave is united with the stimulated wave.

## 6.2 Stability of systematic waves in PLASLA

The aim in this section is to make quantitative study on the stability of the systematic characteristics of the waves generated in PLASLA. In Fig. 17, we show five waves sequentially measured under the same condition in the same experiment. The waves can be classified into the waves with ten peaks and nine peaks; waves 1, 2, and 5 have ten peaks and waves 3 and 4 have nine peaks. The correlation coefficients among these waves are calculated and shown in Table 2. The results in the table indicate that the coefficients are close to 1, i.e., 0.83-0.97 among the ten-peak waves and 0.84 among the nine-peak waves. On the other hand, the coefficients between the ten-peak waves and the nine-peak waves are found to be very small, i.e., -0.044 to 0.13, where the negative value indicates the anti-phase correlation, while it is very small in the present case. These facts indicate that the waves generated in PLASLA are very systematic and classified into the two groups, i.e., the ten-peak waves and the nine-peak-waves. Therefore, they essentially support the model in Fig. 16, suggesting the additional bifurcation during the transformation to the steady-state oscillation.
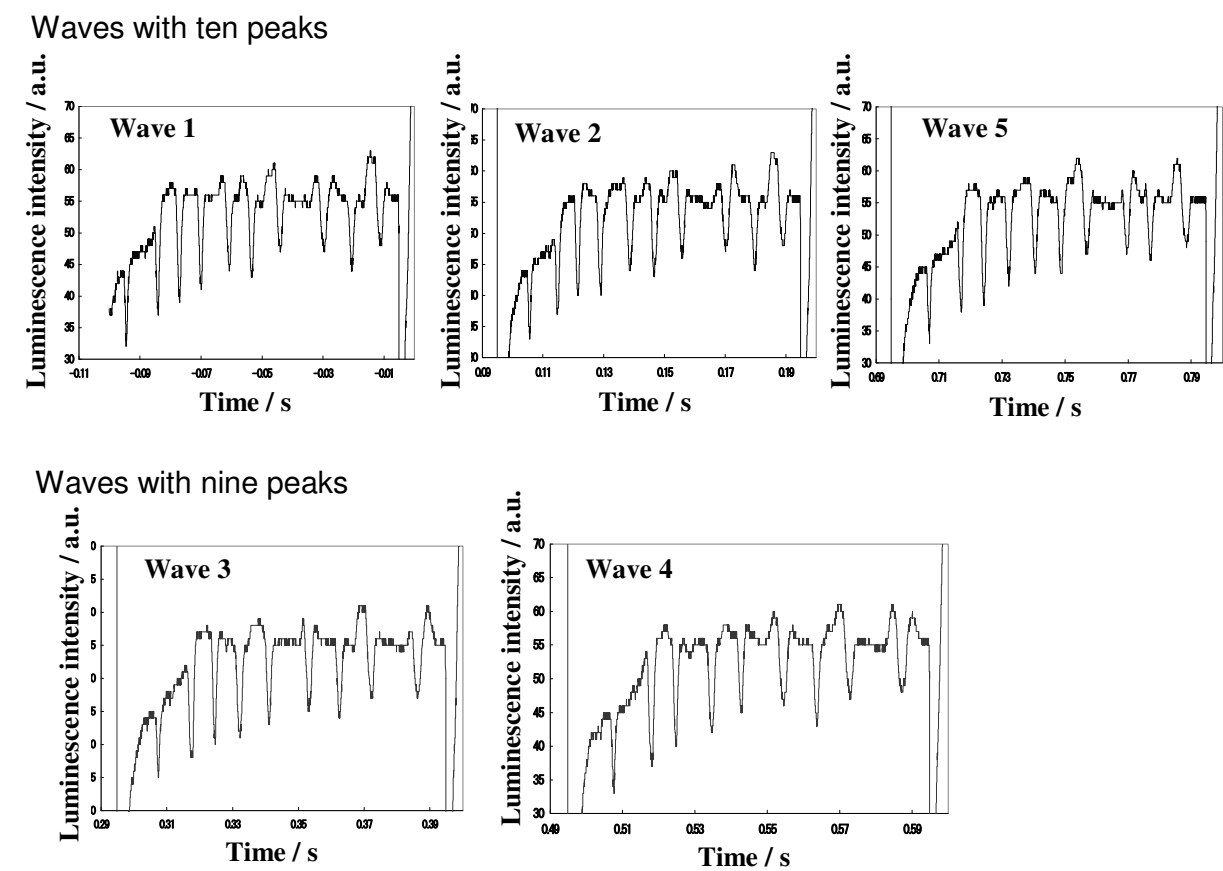
Waves with ten peaks

Waves with nine peaks

Fig. 17. PLASLA waves measured under the same conditions in the same experiment.

|  | Wave 1 (10 peaks) | Wave 2 (10 peaks) | Wave 3 (9 peaks) | Wave 4 (9 peaks) | Wave 5 (10 peaks) |
|---|---|---|---|---|---|
| **Wave 1** (10 peaks) |  | **0.971** | 0.127 | 0.074 | **0.861** |
| **Wave 2** (10 peaks) |  |  | 0.182 | 0.149 | **0.827** |
| **Wave 3** (9 peaks) |  |  |  | **0.840** | 0.051 |
| **Wave 4** (9 peaks) |  |  |  |  | -0.044 |
| **Wave 5** (10 peaks) |  |  |  |  |  |

Table 2. Correlation coefficients between the periods of waves for variations.
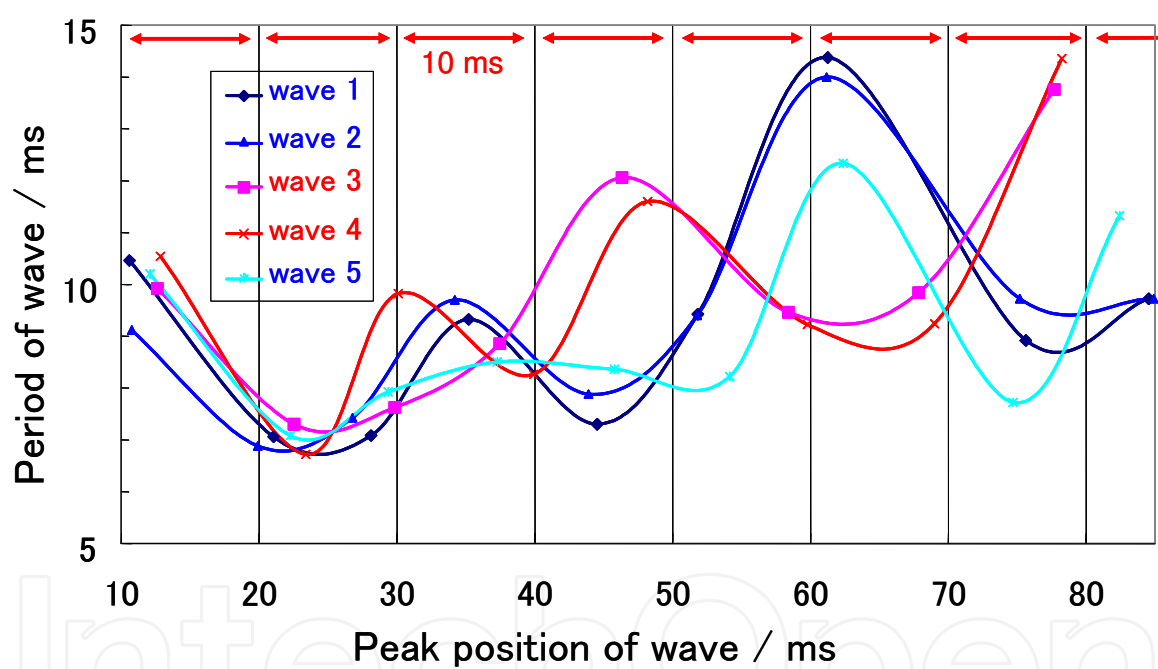


Fig. 18. Periods of waves 1-5 as a function of the peak positions of the waves.

For the study on the bifurcation into the ten-peak wave or the nine-peak wave, we investigate the temporal variations of the correlation coefficients of these five waves, i.e., the time-resolved correlation coefficients of these waves. For the time-resolved correlation coefficients, the periods of these five waves are plotted as a function of time, i.e., the peak positions of the waves, as shown in Fig. 18. In this figure, the abscissa is divided into eight sections by 10 ms. The time-resolved correlation coefficients are obtained by calculating the correlation coefficients of these curves in Fig, 18 in the individual sections of the abscissa and shown in Fig. 19. In Fig. 19, the time resolved correlation coefficients of waves 2-5 with wave 1 are shown, where the coefficients of the waves are normalized to be 1 at 10 ms, i.e., in the section between 10 and 20 ms.
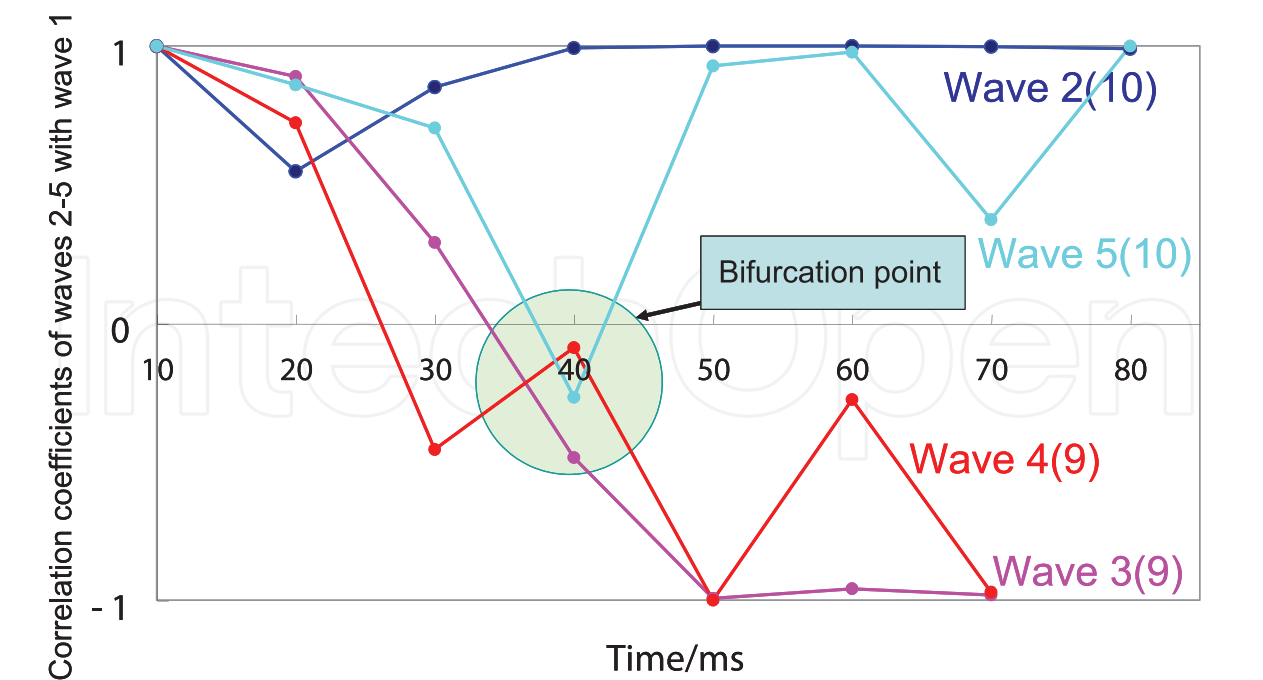
Fig. 19. Time-resolved correlation coefficients of waves 2-5 with wave 1. The numbers in the parentheses are the numbers of the peaks of the waves.
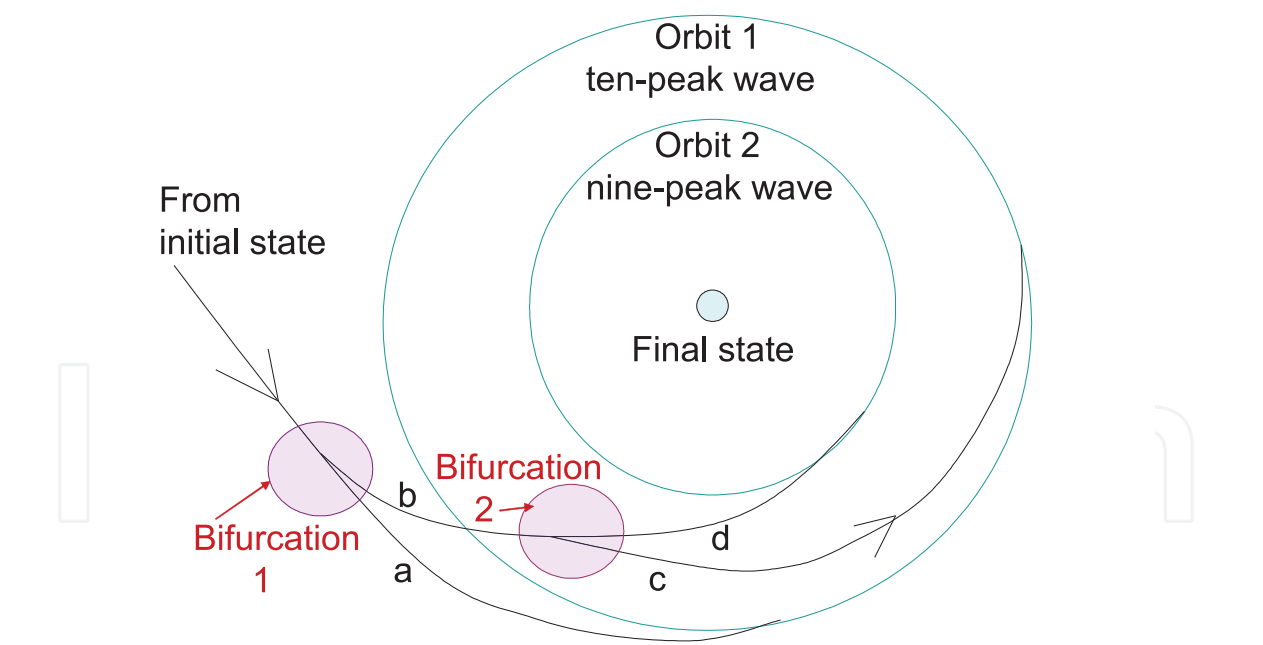


Fig. 20. Schematic illustration of the time evolution of the PLASLA system by the revision of Fig. 16 near the final state.

As shown in Fig. 19, the correlation coefficient of wave 2 decreases a little at 20 ms and after that recovers, approaching to 1. Therefore wave 2 bifurcates to the ten-peak orbit. In Fig. 20,

the revised version of the schematic illustration of the time evolution of the PLASLA system in Fig. 16 is shown. In wave 2, the system goes from the initial state to orbit-1 of the ten-peak wave through bifurcation-1 and path-a.

Another ten-peak wave, wave 5, shows the very different behavior from wave 2, as shown in Fig. 19. The correlation coefficient of wave 5 decreases to zero at 40 ms and recovers to one after that. This behavior of wave 5 will be described as follows with Fig. 20. In wave 5, the system goes from the initial state to orbit-1 of the ten-peak wave through bifurcation-1, path-b, bifurcation-2, and path-c.

Let us study the behavior of the nine-peak waves, waves 3 and 4. As shown in Fig. 19, their correlation coefficients decrease to zero at 40 ms and decease to -1 after that. The behaviors of waves 3 and 4 will be described as follows with Fig. 20. In these waves, the system goes from the initial state to orbit-2 of the nine-peak wave through bifurcation-1, path-b, bifurcation-2, and path-d.

Based on the study in this section, we conclude that systematic temporal waves exist in PLASLA and their behavior is expressed in terms of bifurcation in Figs. 16 and 20. Hence the present mechanism for the temporal waves in PLASLA is found to be closely related to the general concepts for self-organization [Haken, 2006]. We suppose that the plasma chemical processes significantly contribute to the temopral waves in PLASLA, which will be discussed in Section 6.4. Self-organization through chemical processes is known in various systems. For instance, we found that the periodic pulse waves are formed in laser-induced aerosol formation in gaseous $CS_2$, calling it aerosol burst, and studied it experimentally and theoretically [Matsuzaki, 1994].

## 6.3 Effect of electrodes potential on PLASLA

It is of great interest to study the factors, which control the systematic temporal waves in PLASLA. The potential between the electrodes will be one of the important factors. In this section, we study the effect of the potential between electrodes on the systematic temporal waves in PLASLA.

In Fig. 21, the effect of the potential between the electrodes on the growth and decay rates of the amplitude of the front wave is shown. Both rates are constant under the threshold potential and steeply increase over it.

In Fig. 22, we study the effect of the potential between the electrodes on the growth rate of the amplitude of the stimulated wave. The growth rate of the amplitude of the stimulated wave decreases with an increase in the potential between the electrodes. As shown in the figure, the best fit function is the linear function with the negative slope, giving the good correlation coefficient, i.e., $R^2=0.97$.

Thus it is found that the potential between the electrodes affects the front wave and the stimulated wave. Hence the potential is regarded as the significant factor, which controls the waves of PLASLA. This fact will be approved, since the chemical reactions in PLASLA will be affected by the potential through the change in the kinetic energy of electrons. Yet, the mechanism for the potential effect seems to be not simple, since the dependence on the potential is quite different in these waves.

The potential dependence of the front wave suggests that the change in the front wave occurs as the plasma phase transition. The increase in the kinetic energy of electrons does not linearly enhance the front wave but cause the plasma phase transition. That is, while the increase in the electron energy will increase the significant chemical species in the plasma, the plasma phase does not change under the threshold and the phase transition drastically takes place over the threshold. The potential dependence of the front wave will be closely related to this mechanism.

On the other hand, this kind of phase transition seems to be not related to the potential dependence of the stimulated wave. While some assumptions for the mechanism of the anti-correlation between the growth rate of the amplitude of the stimulated wave and the potential between the electrodes can be proposed, here we will discuss the following one, which we consider most probable. That is, the increase in the plasma species interrupts the chemical processes enhancing the stimulated wave. For example, when the chemical processes for the stimulated wave are composed of the chemical reactions by neutral species, they must compete with the ionic chemical processes by the plasma species. As a result, the growth of the stimulated-wave amplitude will be suppressed by the increase in the potential between electrodes.
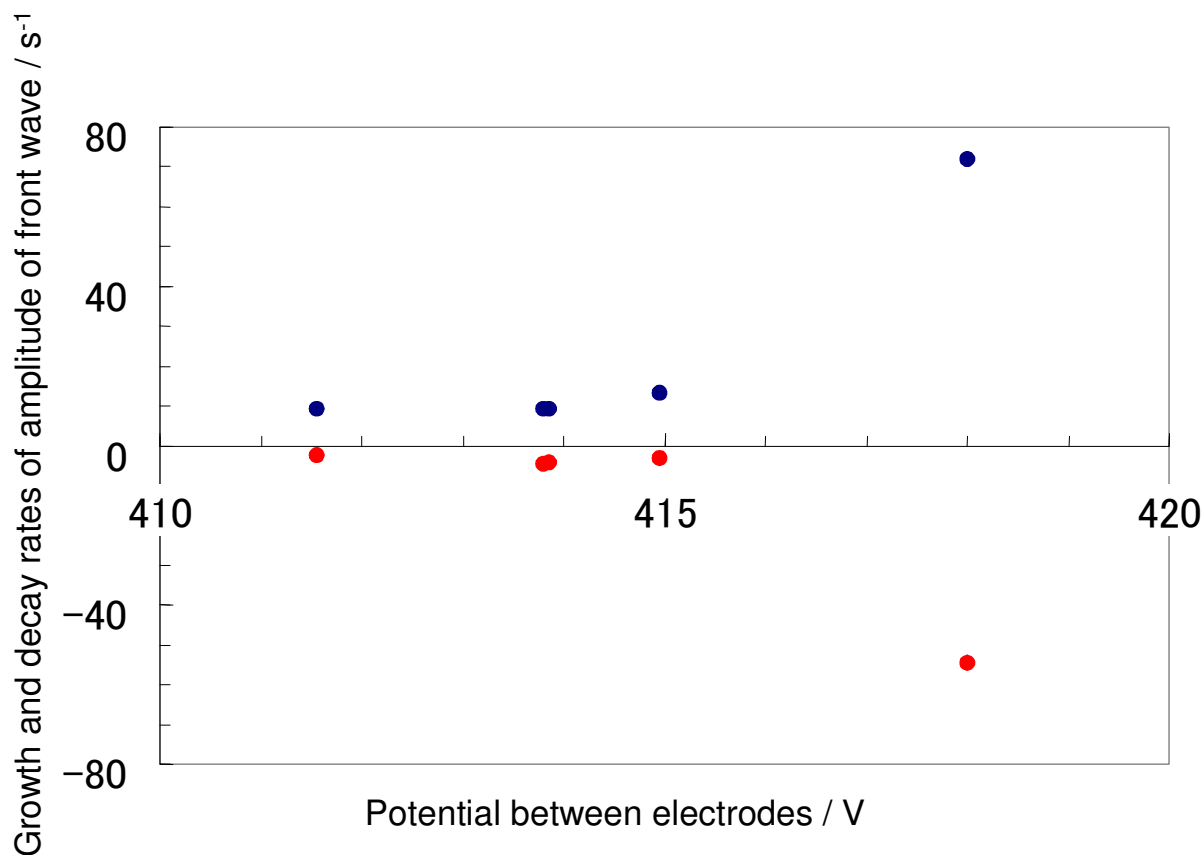


Fig. 21. Growth and decay rates of the amplitude of the front wave as a function of potential between electrodes. Blue: growth rate, red: decay rate.
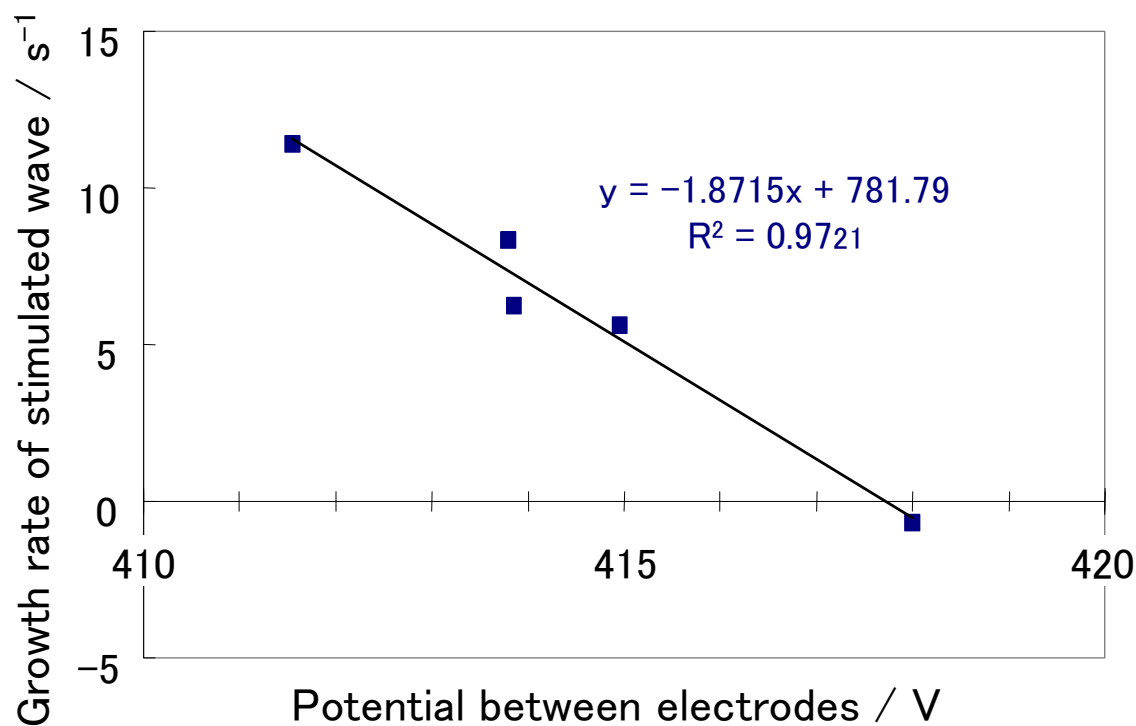
Fig. 22. Growth rate of the amplitude of the stimulated wave as a function of potential between electrodes. In the attached equation, which is the best-fit function, y and x are the growth rate of the amplitude of the stimulated wave and the potential between electrodes, respectively. $R^2$ is the correlation coefficient of the best-fit function.

### 6.4 Theoretical discussion on the temporal waves in PLASLA

On the basis of the experimental study described in sections 6.1-6.3, we have been able to confirm that the systematic temporal waves are formed in PLASLA and deduce the model for the waves. The model is that, as schematically shown in Figs.16 and 20, the front wave is generated just after the laser ablation, inducing the stimulated wave and combining with it to form the stable united wave after that. It has been confirmed that these wave transformations are nonlinear processes. In this section, we will investigate this experimentally deduced model by a theoretical approach. For the approach, we assume that these waves are closely related to the chemical processes in PLASLA, i.e., they are a kind of chemical waves.

In the present theoretical study, we assume that the PLASLA luminescence is mainly due to the luminescence from $C_2^+$, since the analysis of the time-resolved spectra of the PLASLA

luminescence in the previous study suggests that $C_2^+$ ion is one of the most significant species in PLASLA. Hence, for the investigation on the temporal dependence of the PLASLA luminescence, we study the time dependence of the $C_2^+$ concentration in the present theoretical approach:

As shown in Eqs. (1)-(5), essentially, the following five chemical processes will be relevant to the present approach:

$$Cu + e \rightarrow Cu^+ + e \tag{1}$$

$$Cu^+ + CF_4 \rightarrow Cu + CF_4^+ \tag{2}$$

$$CF_4^+ + CF_4 \rightarrow C_2^+ + 4F_2 \tag{3}$$

$$C_2^+ + CF_4 \rightarrow C_3^+ + 2F_2 \tag{4}$$

$$C_2^+ + e \rightarrow C_2 \tag{5}$$

Here, $k_1$ and $-k_5$ denote the rate constants of the processes in Eqs. (1)-(5), respectively. We have the following differential equations for the chemical processes in Eqs. (1)-(5), as shown in Eqs. (6)-(8):

$$d[Cu^+]/dt = k_1[Cu] - k_2[Cu^+][CF_4] \tag{6}$$

$$d[CF_4^+]/dt = k_2[Cu^+][CF_4] - k_3[CF_4^+][CF_4] \tag{7}$$

$$d[C_2^+]/dt = k_3[CF_4^+][CF_4] - k_4[C_2^+][CF_4] - k_5[C_2^+][e] \tag{8}$$

In these equations, parentheses [ ] denote the concentrations of the species; e.g., $[C_2^+]$ indicates the concentration of $C_2^+$. We have Eq.(9) from Eqs.(6)-(8):

$$d^2[C_2^+]/dt^2 = k_3[CF_4]\{ k_2[Cu^+][CF_4] - (( k_3+k_4)[CF_4] + k_5[e]) [CF_4^+]\} + (k_4[CF_4] + k_5[e])^2[C_2^+] \tag{9}$$

For $[Cu^+]/[CF_4^+] = \{( k_3+k_4)[CF_4] + k_5[e]\}/(k_2 [CF_4])$, Eq. (9) is transformed into Eq. (10):

$$d^2[C_2^+]/dt^2 = \omega^2[C_2^+] \tag{10}$$

Here $\omega$ is expressed in terms of Eq. (11):

$$\omega = k_4[CF_4] + k_5[e] \tag{11}$$

Then we have the solution of Eq. (10) as follows:

$$[C_2^+] = [C_2^+]_0 \exp(\pm\omega t) \tag{12}$$

Here $[C_2^+]_0$ is the $C_2^+$ concentration just after the laser ablation. Since $\omega \geq 0$ in Eqs. (11) and (12), it is found that the concentration of $C_2^+$, which is one of the most significant species in the PLASLA luminescence, decays and/or grows exponentially and never stably oscillates with time at a frequency of $\omega$ in Eq. (11) under the condition of $\{[Cu^+]/[CF_4^+]=\{(k_3+k_4)[CF_4]+k_5[e]\}/(k_2 [CF_4])\}$. For instance, the formula of $\{[C_2^+]\propto[\exp(\omega t)-\exp(-\omega t)]\}$, which is one of the possible solutions, indicates that $[C_2^+]$ simply increases with time.

The result in Eq. (12) suggests that the oscillation is unstable and gradually quenching to a none-oscillating final state, which is not a limit-cycle. Therefore, the present theoretical results suggest that the oscillations in the models in Figs. 16 and 20, which have been deduced from the present experimental results, are not stable and will finally disappear. As for this discrepancy, since the present theoretical model is very simplified, its result might be inadequate for discussing the experimental results. For instance, the present theoretical model includes no spatial transference term, which is often the significant factor in self-organization process. In addition to the improvement of the theory by taking account of the spatial terms, the study on the evident correlation between the PLASLA discharge patterns and the temporal waves might be of great interest. Furthermore, we might need to use more complicated chemical processes for the theoretical study. Besides, we might need to study the temporal changes in other chemical species besides $C_2^+$. For instance, the significance of $CF_3$ and anions is suggested [Kiss & Sawin, 1992; Stoffels et al., 1998], as well as C and $C_2$ [Jung et al., 2006].

While Figs. 16 and 20 simply describe the transformation of the system from the initial state to the final oscillating state, more details of this process have been able to be expressed in terms of the front wave and the stimulated wave, as a result of the present experimental study. In particular, it is significant to note that these waves are due to the nonlinear processes with the exponential growth and decay and that their behaviours are not necessarily same for the common parameters such as the potential between electrodes. For example, the different behaviours of the waves for the electrode potential in Figs. 21 and 22 suggest that the processes controlling these waves are not necessarily same, as discussed previously. In spite of the fact, these waves are finally combined to be a united wave.

## 7. Conclusion

In the present article, first, we have reviewed PLASLA (plasma switching by laser ablation) on the basis of our previous papers. In the review, we have introduced the PLASLA phenomenon, the method for the PLASLA formation, the product materials, the properties of PLASLA, and the interaction with a magnetic field. In particular, the significance and promise of PLASLA in materials science have been pointed out. Besides the review, the new original study on PLASLA has been described. In the study, we have investigated the spatial patterns and the temporal waves of PLASLA. Since plasma is a nonlinear process and many interesting ordered structures are known in the spatial and temporal patterns of plasma, the present study will be of great interest.

First we have studied the PLASLA discharge patterns with various target metals. Based on the discharge patterns, the target metals are classified into three groups having the different electronic configurations: Groups-1, -2, -3. In particular, peeling off of the sheaths is clearly observed in the metals of Group-3. Furthermore, for Cu and Ti targets, the luminescence intensity distributions on the electrodes are found to be different outside the reaction site. These facts are due to the competition of the plasma ionic reactions with the neutral chemical reactions in Group-3 metals.

Next, we have analyzed the PLASLA discharge pattern with a Cu target more in detail, as well as those of the DC-plasma and CuF chemiluminescent reaction. In DC-plasma, the

luminescence intensity constantly decreases from the cathode to the anode. Besides, it is found that the unquenched, stable sheath surrounds the cathode. As for the anode, various cases are observed; the sheath appears only in the inside, only in the outside, and in the both sides of the anode, depending on its parts. In PLASLA, the plasma luminescence intensity is much more quenched between the electrodes, where the inside is the side between the electrodes. In particular, the quenching is very large near the inside on the cathode. The sheath appears only in the outsides on the cathode and the anode and is largely, completely in many cases, quenched in the insides of the both electrodes. The characteristic discharge patterns in PLASLA are due to the chemical reactions occurring in the whole region between the electrodes.

Then we have studied the product materials attached to the electrodes for various target metals. As the common results for these metals, it has been found that the yields of black-coloured materials are evidently greater in the anode than in the cathode. Furthermore they are evidently greater in the reaction side of the both electrodes, i.e., the site including the laser-ablation target and surrounded by the electrodes, than in another side, i.e., the sites outside the reaction site. As for target metals, the yield of the black-coloured materials is highest in the Group-1 metals, middle in the Group-2 metals, and lowest in the Group-3 metals. Furthermore the white-coloured materials, which are supposed to be the products of the chemical processes competing with PLASLA chemical processes, are yielded in the metals of Groups-2 and 3, while no white materials are yielded in the Group-1 metals.

After that, we have analyzed the transient signals of PLASLA with various target metals. It is found that the rise of the PLASLA pulse is classified into two types: Type-A and Type-BC. The simulation with the simple model has demonstrated that the rise of the PLASLA pulse moves from Type-A to Type-BC with the delay of the plasma luminescence from the laser ablation. The delay depends on the electronic configurations of the target metals. While the decay rate of decay B and the rise rate of decay C depend on the target metals, the plot of the logarithmic value of the former as a function of the latter shows the good linear correlation with the positive slope. The feature of the PLASLA pulse extinction suggests that the PLASLA luminescence signal decays in the two steps probably with the sequence of two exponential decays.

Finally, we have investigated the temporal waves in PLASLA. The study has revealed how the PLASLA system moves on after the laser ablation. After the laser ablation, the front wave is generated, grows and then decays exponentially. With the decay of the front, the stimulated wave grows exponentially. Finally, the front wave and the stimulated wave are combined to be a united wave. The amplitude of the united wave is almost constant with a slight increase. The present theoretical study with a simple model has suggested that the oscillation of the luminescence intensity of $C_2^+$ is not stable and will finally disappear. Since the present theoretical model might be too simple, we need to improve the present theory. We suppose that the temporal waves are due to the chemical processes. While the potential between the electrodes are regarded as a significant parameter to control the chemical processes in PLASLA, the dependence on the potential is found to be different in the front and stimulated waves; the amplitude of the stimulated wave is constant under the threshold potential and steeply increases over it, while the one of the stimulated wave decreases with the

potential. For the fact, we have supposed that the front wave is due to the ionic plasma reactions enhanced by the potential, while the chemical reactions promoting the stimulated wave compete with the ionic chemical reactions enhanced by the potential. Furthermore, we have supposed that the threshold observed in the front wave is due to the nonlinearity of the ionic plasma reactions.

## 8. Acknowledgment

## 9. References

Lieberman, M. A. & Lichtenberg, A. J. (2005).*Frontmatter, in Principles of Plasma Discharges and Materials Processing, second Edition,* John Wiley & Sons, Inc., ISBN 9780471720010, Hoboken, NJ, USA

Nakano, Y.; Kawai, H.; Takenaka, T.; Hon, S.; Mizuguchi, T. & Matsuzaki, A. (2010).CuF-Chemiluminescent Reaction and Plasma Switching by Laser Ablation in the Gaseous Cu-$CF_4$ System and Their Interactions with Magnetic Field. *Journal of Physical Chemistry A,* Vol.114, No.18, (May 2010), pp. 5601-5617, ISSN 1089-5639

Tanaka, H.; Hirano, T. & Matsuzaki, A. (2003).Gas-phase Chemical Reaction of Laser Ablated Copper Atom with Carbon Tetrafluoride in Electric and Magnetic Fields. *Transaction of the Materials Research Society of Japan,* Vol.28, No.2, (June 2003), pp. 275-278, ISSN 1382-3469

Tanaka, H.; Hirano, T. & Matsuzaki, A. (2004).Gas-phase Chemical Reaction of Laser Ablated Copper Atom with Carbon Tetrafluoride in Electric Field: Plasma Switching by Laser Ablation (PLASLA). *Transaction of the Materials Research Society of Japan,* Vol.29, No.8, (December 2004), pp. 3399-3402, ISSN 1382-3469

Tanaka, H.; Hirano, T. & Matsuzaki, A. (2003).New Metal Catalytic Process of Gas-Phase Ionic Reaction : PLASLA (Plasma Switching by Laser Ablation), *Proceedings of 7th Meeting of Symposium on New Magneto-Science*, pp. 35-42, Tsukuba Magnet Laboratory, National Institute of Materials Science, Tsukuba, Japan, November 5-7, 2003

Haken, H. (2006). *Information and Self-Organization: a Macroscopic Approach to Complex Systems,* Springer, ISSN 0172-8379, Berlin Heidelberg, Germany

Matsuzaki, A. (1994).Nonlinear Dynamics in Laser-Induced Aerosol Formation from Vaporized $CS_2$: Period Fluctuation in Aerosol Burst. *Journal of Molecular Structure (Theochem)*, Vol.310, (July 1994), pp. 83-93, ISSN 0166-1280

Kiss, L. D. B. & Sawin, H. H. (1992).Evaluation of $CF_4$ Plasma Chemistry by Power Modulation. *Plasma Chemistry and Plasma Processing,* Vol.12, No.4, (December 1992), pp. 523-549, ISSN 0272-4324

Stoffels, W. W.; Stoffels, E. & Tachibana, K. (1998).Polymerization of Fluorocarbons in Reactive Ion Etching Plasmas. *Journal of Vacuum Science Technology A,* Vol.16, No.1, (January/February 1998), pp. 87-95, ISSN 0734-2101

Jung, T. Y.; Kim, D. H. & Lim, H. B. (2006).Molecular Emission of $CF_4$ Gas in Low-pressure Inductively Coupled Plasmas. *Bulletin of Korean Chemical Society,* Vol.27, No.3, (March 2006), pp. 373-376, ISSN 0253-2964

**Materials Science and Technology**

Edited by Prof. Sabar Hutagalung

Materials are important to mankind because of the benefits that can be derived from the manipulation of their properties, for example electrical conductivity, dielectric constant, magnetization, optical transmittance, strength and toughness. Materials science is a broad field and can be considered to be an interdisciplinary area. Included within it are the studies of the structure and properties of any material, the creation of new types of materials, and the manipulation of a material's properties to suit the needs of a specific application. The contributors of the chapters in this book have various areas of expertise. therefore this book is interdisciplinary and is written for readers with backgrounds in physical science. The book consists of fourteen chapters that have been divided into four sections. Section one includes five chapters on advanced materials and processing. Section two includes two chapters on bio-materials which deal with the preparation and modification of new types of bio-materials. Section three consists of three chapters on nanomaterials, specifically the study of carbon nanotubes, nano-machining, and nanoparticles. Section four includes four chapters on optical materials.

**How to reference**

In order to correctly reference this scholarly work, feel free to copy and paste the following:

Ryosuke Hasegawa, Kazunori Fukaya and Akiyoshi Matsuzaki (2012). Plasma Switching by Laser Ablation, Materials Science and Technology, Prof. Sabar Hutagalung (Ed.), ISBN: 978-953-51-0193-2, InTech, Available from: http://www.intechopen.com/books/materials-science-and-technology/plasma-switching-by-laser-ablation

# INTECH
open science | open minds